

Spectral Background Subtraction Errors in Infrared Field Measurements Made with Fourier Transform Spectrometers

H.C. Schau

Raytheon Systems Company

PO 11337

Tucson, AZ

85734-11337

hcschau@west.raytheon.com

Copyright 1999 Raytheon Systems Company

Abstract: The measurement of infrared spectra of tactical aircraft has been a mainstay in providing signatures for both analysis and simulation to missile seeker designers for many years. Whereas many modern air vehicles have seen their intrinsic infrared signatures reduced over time, the variation in atmospheric backgrounds remains a natural phenomenon which has placed limitations on both operational characteristics of field measurement and the accuracy with which weak targets may be characterized. This paper presents a heuristic method for reducing errors introduced by natural variations in backgrounds in spectral background subtraction. The motivation behind the new technique is discussed as well as the theoretical development of the new technique to reduce spectral background induced errors. An example showing measurements of a small model aircraft are presented with both corrected and uncorrected results. These results are contrasted with apriori expectations of the aircraft signature to provide specific instances when uncorrected background induced errors can limit the measurement accuracy of weak or suppressed air vehicles.

INTRODUCTION

The application of Fourier Transform Spectroscopy (FTS) for making field measurements of infrared sources has been commonplace for over thirty years. The merits of FTS instrumentation are well documented [1], and both custom-made and commercial systems have been available for some time. Applications of FTS technology are as diverse as the characterization of air pollution [2], smoke stack effluents [3-4], and military target signature characterization for missile seeker development [5]. Common to all these applications is the need to estimate the apparent (through the intervening atmosphere) source spectrum, or the apparent source spectral contrast between source and background. The latter is often desired when measurements are to be used in the analysis of missile seekers which employ target to background contrast rather than target intensity alone.

In the past, targets such as military aircraft have possessed higher signatures (measured in units of radiant intensity) than any natural background, so that errors in background subtraction were insignificant relative to the target strength. Today, as military targets have become relatively lower in intensity, background subtraction errors have become a major concern. This is true also in remote sensing studies where for example, increased sensitivity in chemical detection is sought causing fluctuations in backgrounds to often be the limiting feature of the technique[6-7]. Several techniques exist for minimizing background noise contribution. FTS instruments can be converted to imaging spectrometers so that only pixels on the target are counted in the overall interferometer signal. This certainly reduces the background contribution, but can introduce other problems such as system complexity and cost, increased signal processing burden, and require more complex calibration procedures. Another method for reducing background variations is to carefully choose measurement locations and methodologies so that background variations are minimized. This is often impractical due to operational constraints. It is therefore important to develop techniques for minimizing background subtraction errors from conventional single field of view (FOV) FTS instruments under conditions significantly general that they may continue to be employed in field measurements.

FTS SPECTRAL CONTRAST MEASUREMENTS

Figure 1 illustrates two typical measurement scenarios. We consider two limiting extremes in our discussion; one for an optically opaque target such as an aircraft, the other for an optically thin target such as a low density plume. In actuality, nearly all targets fall somewhere between these limits, aircraft have plumes which are not strictly optically thin, and larger plumes such as smokestacks are not formally optically thin but rather interact with the background radiation propagating through them. The division of opacity into optically thin and optically thick approximations does serve to provide useful insight into the background subtraction problem. We also make the approximation that the radiative transfer equations may be approximated as the integral of a source times a transmission, integrated over wavelength plus any path radiance contribution generated by the atmosphere between the observer and source [8-9].

unclassified

Background Subtraction

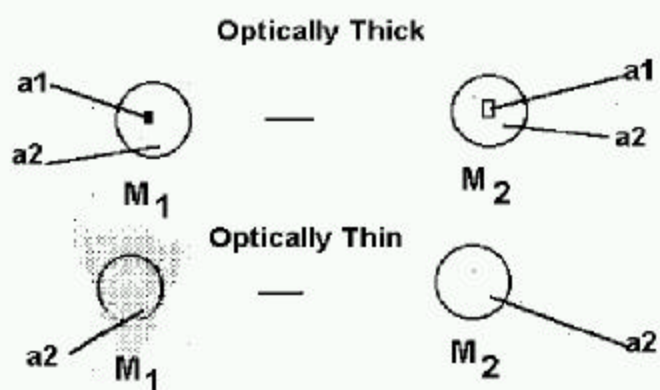


Figure 1

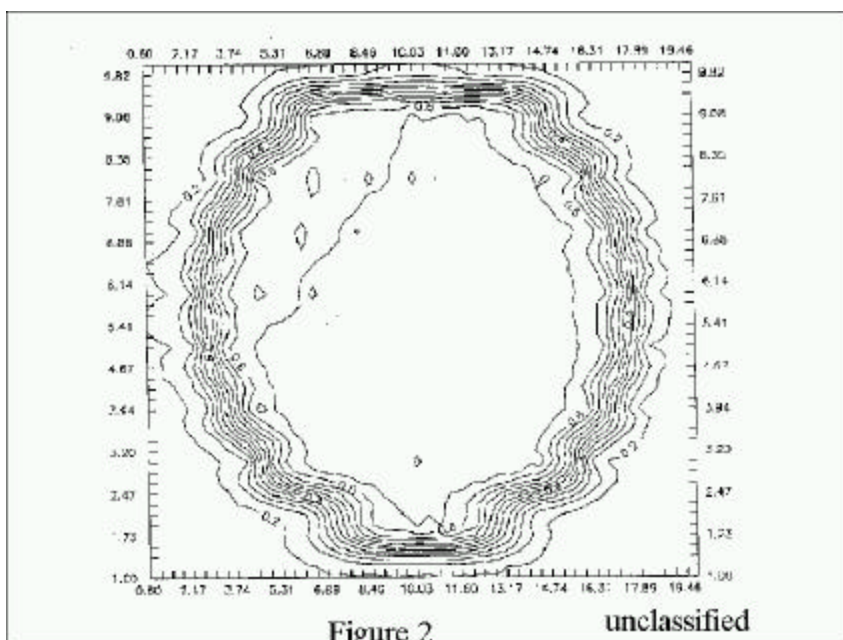


Figure 2

unclassified

Consider the optically thick case of Figure 1, the target signature is (working in engineering units of wavelength rather than spectroscopic units of wavenumber) shown in M_1

$$(1) \quad S_t(\lambda) = \int_{a1} T(\lambda, x, y) S(x, y) dx dy + \int_{a2} B_t(\lambda, x, y) S(x, y) dx dy = T(\lambda) + R_t(\lambda) + B_t(\lambda)$$

where T is the target spectrum passed through the atmosphere and convolved with the spectrometer instrument line shape (ILS). $S_t(\lambda)$ also includes the path radiance R_t , from the observer to the target spatially over the target area, a term which includes atmosphere self emission and scattered radiation. B_t is the background around the target. Background radiation behind the target is occluded by the target since the target is considered optically thick or opaque. S is the instrument spatial field of view function. An example of an actual field of view for a FTS is shown in Figure 2. It is the variable response as shown in Figure 2 rather than an idealized top-hat spatial response which makes conversion of data calibrated in irradiance into radiance and vice versa difficult. Using conventional radiometry [10], target radiant intensity I in W/sr is related to the irradiance E in W/cm² and range R in cm via the equation

$$(2) \quad I = R^2 E$$

which assumes the target is at great enough range that it may be approximated as a point source. The radiance L in W/cm²-sr is related to the irradiance by the relation

$$(3) \quad E = \Omega L$$

where Ω is the source angular subtense. When the radiance of a background is being considered, the angular subtense is the instrument field of view, a function which is difficult to characterized accurately. For this reason spectral calibrations for both irradiance and radiance are often required if both irradiance (or radiant intensity) and radiance are desired. Since discussions here are independent of calibration type, we will not address whether the spectrum are in irradiance or radiance units.

The background M_2 , in Figure 1 is similar to equation (1)

$$(4) \quad B(\lambda) = \int_{a1} B_1(\lambda, x, y) S(x, y) dx dy + \int_{a2} B_2(\lambda, x, y) S(x, y) dx dy = B_1(\lambda) + B_2(\lambda)$$

The spectral contrast function is then often defined as

$$(5) \quad S_c(\lambda) = S_t(\lambda) - B(\lambda) = T(\lambda) + R_t(\lambda) + B_t(\lambda) - B_1(\lambda) - B_2(\lambda).$$

If the background is homogenous such that $B_1(\lambda) = B_2(\lambda)$, then the spectral contrast function (5) is the difference between the apparent target plus the path radiance and the background it occludes. Since the path radiance from the observer to the target is in both contributions, it cancels, leaving the target spectrum minus the background contribution from target to infinity . In the case of optically thin targets, there is essentially no $a1$ and an analogous equation to (5) may be written. In this case, the target is superimposed on the background so that for homogenous backgrounds the entire background over the FOV is both measured and subtracted. Thus for optically thin targets, the spectral contrast is just the apparent source spectrum.

$$(6) S_c(\lambda) = S_t(\lambda) - B(\lambda) = T(\lambda).$$

The chief problem which we face, is that the two backgrounds are never exactly the same. This problem is exacerbated by the fact that targets are typically small (we will discuss optically thick targets in the remainder of this paper, the discussion is equally pertinent to optically thin targets since their integrated signature is typically considerably less than the corresponding background), thus resulting in a weak signal superimposed on a large background contribution. This can create a situation of large error when backgrounds do not subtract exactly, the resulting error term can dominate the target signature.

Before we proceed further with our discussion of reducing background subtraction errors, we must briefly discuss an alternate form for equation (5). The spectral contrast function is sometimes defined as

$$(7) S_c(\lambda) = T(\lambda) - B_o(\lambda) ,$$

the difference between the apparent target spectrum and the background behind the target where in this case the path contribution from observer to target is in the background term only. In this case, an estimate of the path radiance $P(\lambda)$ contribution is usually required since it does not cancel and must be accounted for separately. It is often assumed that $P(\lambda)$ is proportional to the background so that forming the difference

$$(8) S_c(\lambda) = S_t(\lambda) - \alpha B(\lambda)$$

would provide an estimate of this spectral contrast function. The parameter α is found in a variety of ways, one common approach is to consider the difference shown in equation (8) for a variety of α 's. By looking in a strong atmospheric absorption window such as the CO_2 absorption window around 4.3μ , it can be assumed that any resulting spectral energy is a result of the path radiance. Then the parameter α can be adjusted to just cancel all contributions in this spectral region and make the resulting spectral contrast equal to the background. This process also has spectral background subtraction errors in it; the differences of the target and background spectra, and the assumption that the path radiance to the target is proportional to the background spectrum. Depending on the range to the target and the spectral band, this assumption is more or less valid. Figure 3 shows a typical measured background, while Figure 4 displays the path radiance calculated with Lowtran7 [11] for a target 3.5 km away under similar conditions . As can be seen from Figures 3 and 4, the assumption that the path radiance to the target is proportional to the background has validity.

Measured Background

Note reflected Solar Radiation @2.3 μ

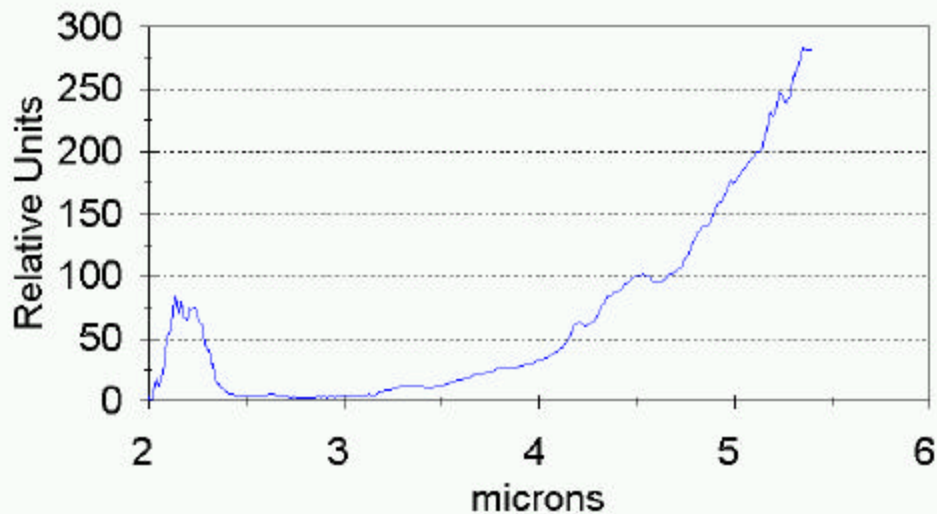


Figure 3

unclassified

Calculated Path Radiance

3.5 km

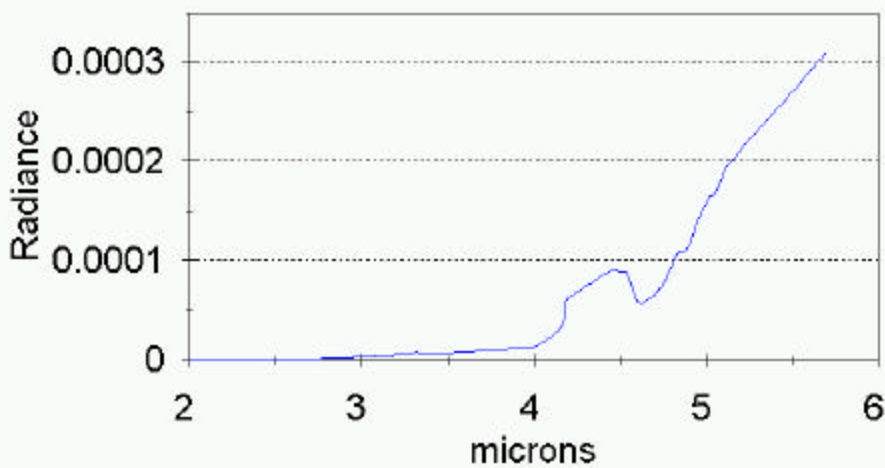
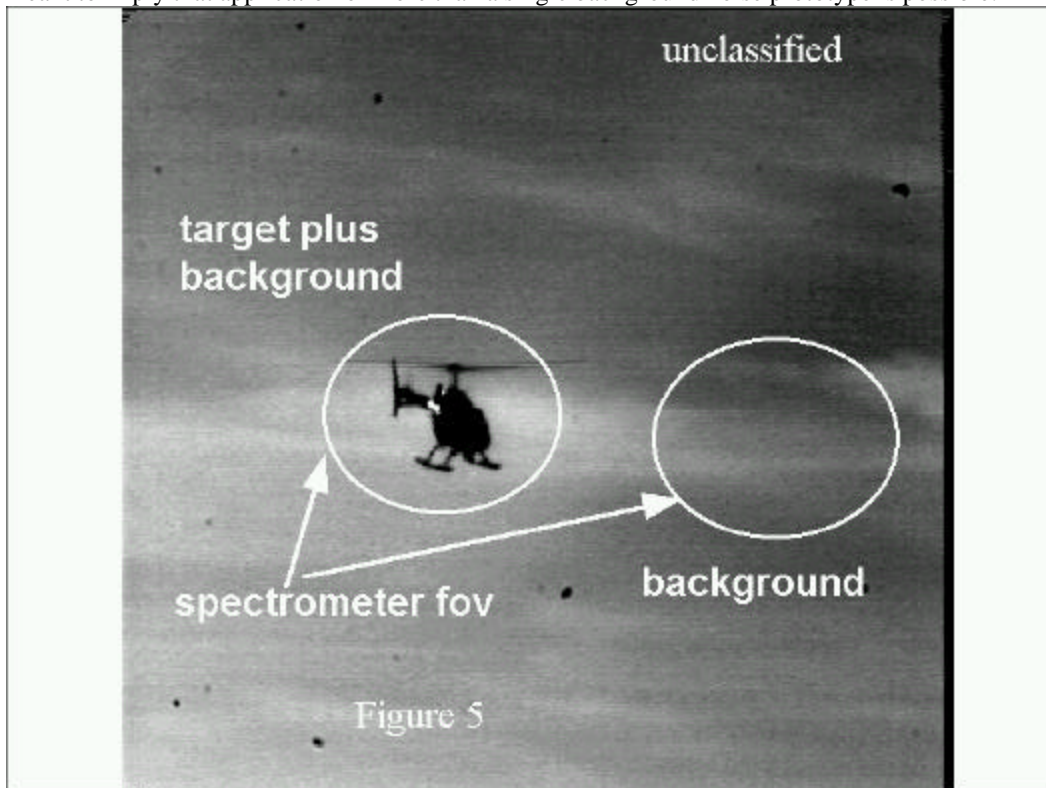


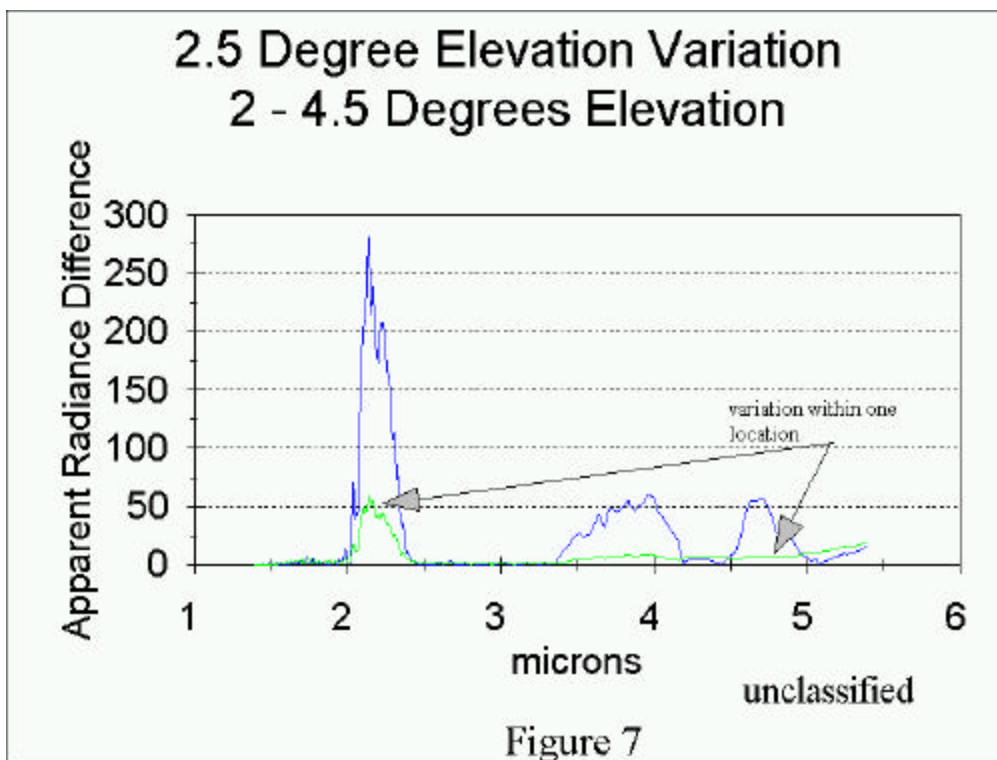
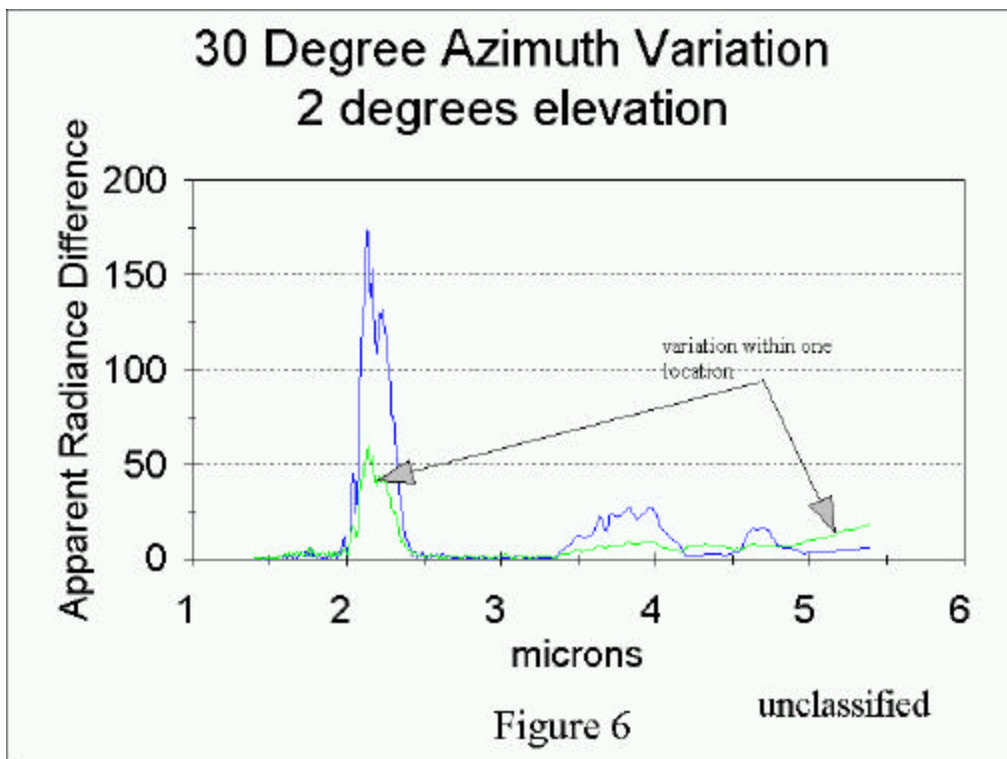
Figure 4

unclassified

Figure 5 presents a visible image of a typical measurement scenario of an aircraft. In cases of hover and flyby, the ideal situation is achieved when a measurement is made of the target plus background, followed by removing the target from the background and measurement of the background alone. In this case, the subtraction errors are caused by the temporal background change over the measurement times, typically a few minutes, and the difference of the occluded background from the rest of the background and the target. However, for a variety of reasons, it is usually impractical to attempt such a measurement. In flyby

measurements, it is difficult to return to the same position in the sky where the initial measurement was made since the spectrometer is typically tracking the target; in hovers there is usually not enough time for the target to fly away from the position where measurements were made and return a few minutes later to be repositioned. For these reasons, background measurements are typically made as close to the target as possible, in regions of background similar to where measurements were made as shown in Figure 5. As an example of the variations in sky background, consider Figures 6-7. Figure 6 shows the variations in background for two locations 30 degrees apart in azimuth at 2 degrees elevation. Figure 7 displays the difference for a 2.5 degree elevation change from 2 to 4.5 degrees. Shown on both figures is an indication of the variation in one location which is calculated as the average of the differences of spectra at each azimuth and elevation over a period of several minutes. Notice that the spatial variation is considerably greater than the temporal variation over the time period of typical measurements. Central to our concept of reducing background variation, is that background variation can be modeled for a given measurement scenario. This is clearly true for blue sky for any likely atmosphere with the variation much like that shown in Figures 6-7. It is beyond the scope of this article to provide details of this assumption, rather the degree to which it may be extended to non-homogenous atmospheres (such as instances when targets fly through cloud edges or terrain appears in the background) and other spectral bands, can be estimated from reference 12. It is likely that in application to non-homogeneous backgrounds, one background prototype might be employed to represent blue sky variation while another would be employed to represent cloud-blue sky or terrain-blue sky variation. In the event a single prototype could not represent background variations, some prior knowledge of the type of background variation for a given measurement must be available (such as off video tape of the measurement process) or the error reduction could be applied for each background prototype and the correct choice based on the error metrics described below. In order to simplify our discussion, we will assume a single background variation prototype can be employed, this in no way is meant to imply that application of more than a single background noise prototype is possible.





Technique For Minimizing Background Subtraction Errors and Estimating Target and Contrast Functions

The technique we propose is intended to minimize background subtraction errors in spectral contrast functions, and, provide estimates of the target spectrum alone (we specifically discuss apparent values, i.e. as passed through the atmosphere). The process makes several assumptions. It first assumes that the path radiance (although we describe these contributions as radiance by convention, we assume all units have been converted to radiant intensity in the remainder of this paper, other units follow similarly) from the observer to the target can be measured or otherwise estimated (or for many practical applications, assumed small enough to be neglected and set to zero). It is also assumed that within the spectral measurement range, there exists an atmospheric absorption band intense enough that no target energy reaches the observer within this band. In this case, we may approximate the radiation in this band as path radiance from observer to target only. These two assumptions place limits on both range and spectral bands. For the applications envisioned here, the 2-12 μ band, this restricts the range to greater than approximately 0.2-0.3 km in normal atmospheres since the CO₂ band at 4.2 μ is a strong absorber. We also assume that some model is available for the spectral shape of the background variations, not the intensity, but the relative weights of the background variations within the measurement spectral interval. As we have seen the relative weighing of the background variations has a similar shape under different circumstances although the intensity can vary considerably. Under these assumptions, the mechanism for reducing measured target and background spectra can be broken down to a five step process.

The first step is to estimate the amount of the FOV which is occluded by the target. As stated previously, this is simply done by considering a strong atmospheric absorption band and assuming we may estimate the components of the spectrum reaching the observer. The simplest assumption is that no target energy reaches the observer and any energy within the band is the result of path radiance between the observer and the target. While path radiance from observer to target is difficult to measure, it can be estimated from atmospheric transmission codes [13-14], particularly if knowledge of the lower atmosphere meteorology is available. In our application of measuring military aircraft at a range of 1-5 km, we typically make the simplest assumption that path radiance can be neglected. This makes the difference in path radiance definitions (equations 5 and 7) unimportant. In applications where path radiance contributions must be taken into account, they may be estimated from atmospheric radiation codes. The degree of obstruction is important in estimating the target not the contrast as we shall see. Thus the effective degree of obstruction is given by

$$(9) \quad A = \frac{\int S_t(I) dI - R_t}{\int B(I) dI}$$

where the integration is over the absorption band chosen, and R_t is the estimated path radiance contribution. In our application we have chosen the 4.195 to 4.296 μ CO₂ absorption band. Examination of equations 1 and 4 reveals that this is simply the ratio of what is perceived as the background contribution in the target measurement (minus the estimated path radiance contribution), to the total background. It must be remembered that there is typically differences between the background in the target measurement and that in the background measurement. Although equation 9 assumes the degree of obstruction is the ratio of the two backgrounds, differences between these necessarily introduce errors in the estimation of A. It has been found that for typical backgrounds A can often be estimated to better than 5 percent which is adequate for our purposes.

The second step is to form a prototype for the background noise or variation, which may be present in the measurement. It is not important to estimate the strength of the variation, only the overall spectral shape. This may be obtained from models, past measurements, or by considering variation in background measurements taken at times and locations near the measurement of interest. All three techniques have been used successfully, perhaps the most direct method is to simply consider several measured backgrounds taken near the measurement of interest and average their differences. The method

chosen usually depends on what information is available. We remark again that this prototype only estimates the relative spectral shape of the background variation, we estimate its strength in a separate step.

The processing follows by first establishing a prototype background which is the measured background corrected for variation between itself and the background in the target measurement. The variation is assumed proportional to the spectral prototype.

$$(10) \quad B_p = B - \gamma P$$

where B is the measured background as described by equation 4, P is the spectral prototype, B_p is the corrected prototype background, and, γ is a strength factor (as yet undetermined) which describes the strength of the background noise or degree of background variation between the background contained in the target measurement and the background measurement. From this corrected background we form a corrected target prototype

$$(11) \quad T_p = S_t - B_p A$$

where T_p is the corrected target prototype, S_t the measured target plus background spectrum described by equation 1, and B_p is corrected background prototype described by equation 10. The corrected prototype spectral contrast function is then defined as

$$(12) \quad S_{pc} = S_t - B_p$$

where S_{pc} is the corrected prototype spectral contrast function and S_t and B_p are as defined previously. Recall that in our applications, path radiance from observer to target is neglected making the distinction between equations 5 and 7 unnecessary. Applications where it must be considered for which the definition of spectral contrast was either equation 5 or 7 would have prototype reconstruction which follow accordingly.

This simple reconstruction provides both corrected target and contrast estimates from the target and background measurements, estimates of the target obstruction, and an estimate of the spectral shape of the background variation. It is observed that the entire reconstruction process is dependent on obtaining an accurate estimate of the parameter γ , the strength of the background noise. This parameter can be estimated by forming the normalized inner product between the corrected prototype target and background variation prototype.

$$(13) \quad e = \frac{\int (T + Ae - AgP) P dI}{\int (T + Ae - Ag\gamma) dI}$$

The justification for this choice of metric is discussed in appendix A. It suffices to remark here, that the actual error between the actual target and the corrected spectral prototype is a broad flat function of the parameter γ . The point where the mean square error (squared difference between the estimated target and actual ,or, alternatively between the background variation the product of γ and the background noise

prototype function) obtains it's minimum is close to the point where $\frac{\int e}{\int g} = 0$. Acceptable performance has been found by simply biasing γ by a small amount from that point.

Examples

A set of synthetic data was prepared to study the effectiveness of the error reduction procedure described above. A measured aircraft target T , and background B , were employed together with measured background variations $N1$ and $N2$, to prepare simulated measured quantities via the equations

$$(14) \quad M = sT + B(1 - \alpha)$$

$$(15) \quad Bkg = B + \beta N2$$

$$(16) \quad P = \frac{N1 + N2}{2}.$$

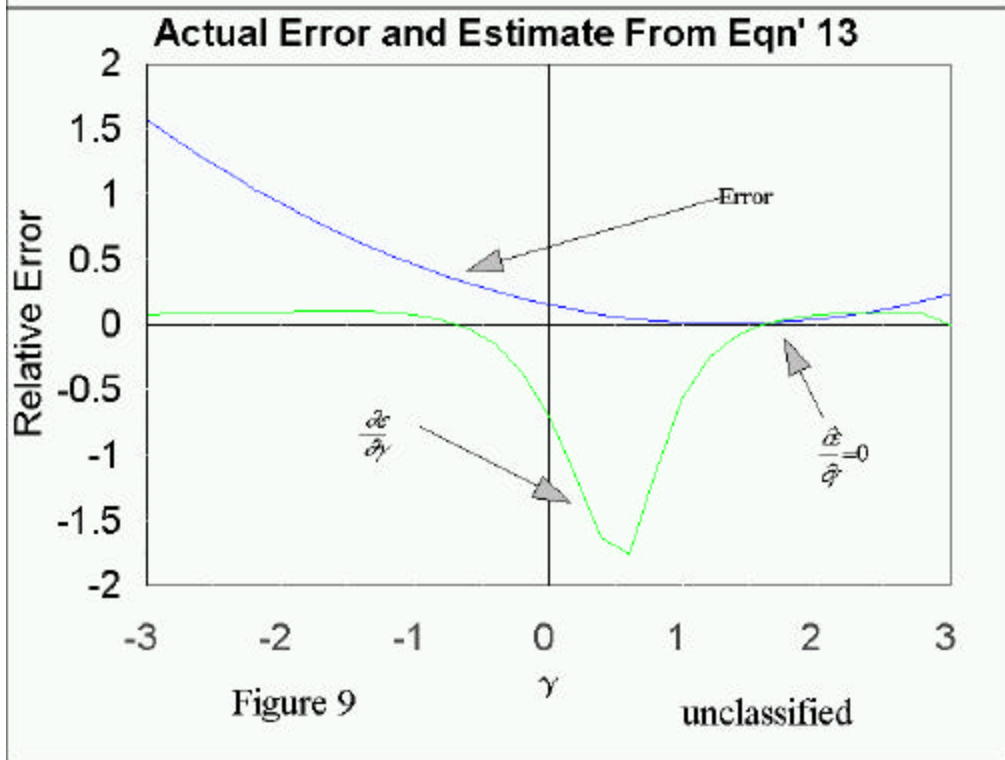
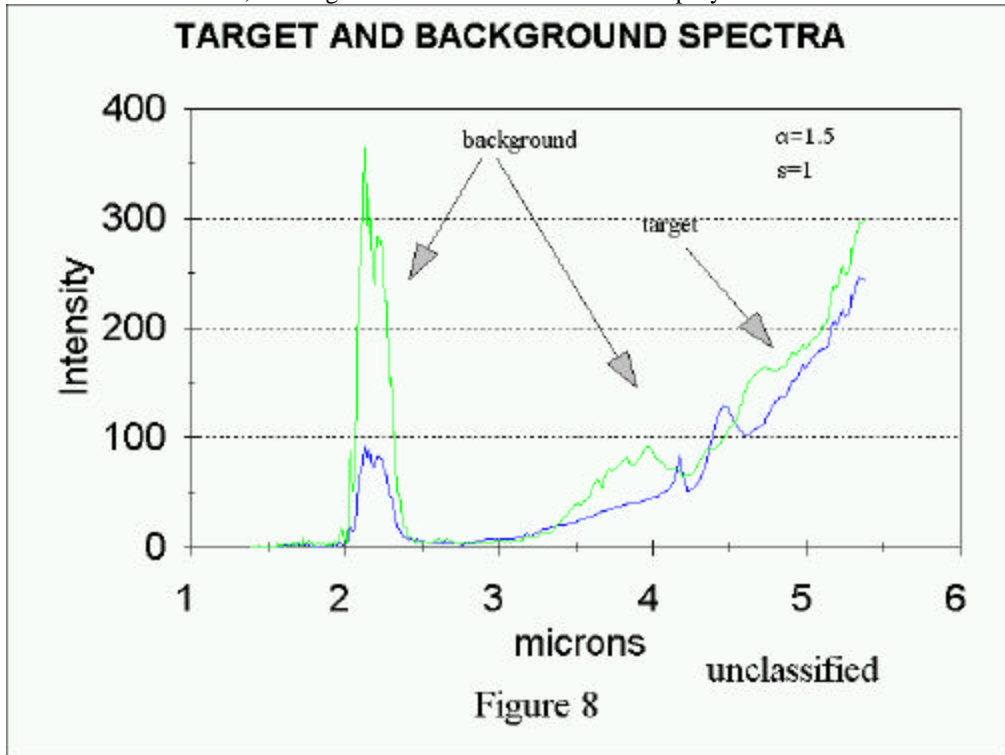
Here M is the measured spectrum with the target in the FOV, Bkg is the measured background with background variation, and, P is the spectral prototype of the background variation. Note that the background noise prototype is similar to the actual background noise used ($N2$), but is not identical. The two measured background variations were averaged to obtain a background noise prototype so that 50% of the prototype is representative of the actual background noise, the other half is different. This is felt to be a realistic representation of the degree of similarity one could expect between the actual background variation (recall these are spectral shapes only, absolute intensity is not required in the prototype, this is taken care of by the parameter γ) and the spectral prototype. The parameter α represents the size of the target, that is, the percent of the FOV that the target obscures, while β represents the overall strength of the background noise. Note that using the equations above the actual target spectrum is given by

$$(17) \quad Act = M - (1 - \alpha)B$$

Figure 8 displays M and Bkg for one set of parameters, while figure 9 shows the mean square spectral error between the estimated target (equation 11) and the actual target (equation 17) as a function of γ . Shown also is the curve $\frac{I_e}{I_g}$. The choice for γ in this example was found to be 1.3 (the curve crosses zero at 1.8 and is biased left by 0.5, see appendix A). Figure 10 shows the estimated target spectrum together with the actual, while figure 11 presents the estimated spectral contrast function developed via equation 12, the actual spectral contrast function, and the conventional spectral contrast function as given by equation 5 ($M - Bkg$).

As yet, we have only considered synthetic data, that is, data synthesized from real measured targets and backgrounds. In such a case we know the answer, but we would also like to contrast the technique with the normal uncorrected method in a real field measurement. A small model aircraft was measured in early summer in a desert atmosphere. Range was nominally .5km, elevation was nominally 20 degrees. Weather at the beginning of the test was blue sky with some clouds, approximately 1 hour later at the conclusion of the test, rain was beginning to fall. A background prototype was formed by measuring backgrounds over a patch of sky where measurements were made, approximately 15 degrees in azimuth and elevation, and averaging the differences. Based on a priori knowledge of the target, a simple model was constructed of the integrated target spectral intensity (W/sr) over the spectral band from 3.8 to 4.7 microns. The background employed for any given target pass was one taken as close in time as the measurement while being in the approximate measurement direction. The target made many passes over a spot .5 km in front of the spectrometer at different headings and hence different aspect angles. The spectrometer tracked the target for approximately ten seconds taking twenty interferograms. The interferogram closest to the crossover point was chosen. A background for that run was usually taken next. It was often impossible to follow the same trajectory as the target run since it was unknown at that time. The backgrounds were taken when the target turned around for the next run which did not allow review of which interferogram was closest to crossover. For this reason, backgrounds were not always measured near the measurement point. The variation in target elevation was approximately 10 degrees and variation in measurement aspect angle

could be plus or minus 5 degrees due to variations in the targets heading which caused it to miss the crossover point. Due to both equipment and time limitations, on occasion no backgrounds were taken for a run. In these instances, a background from another run was employed.



Actual and Estimated (eqn' 11) Target

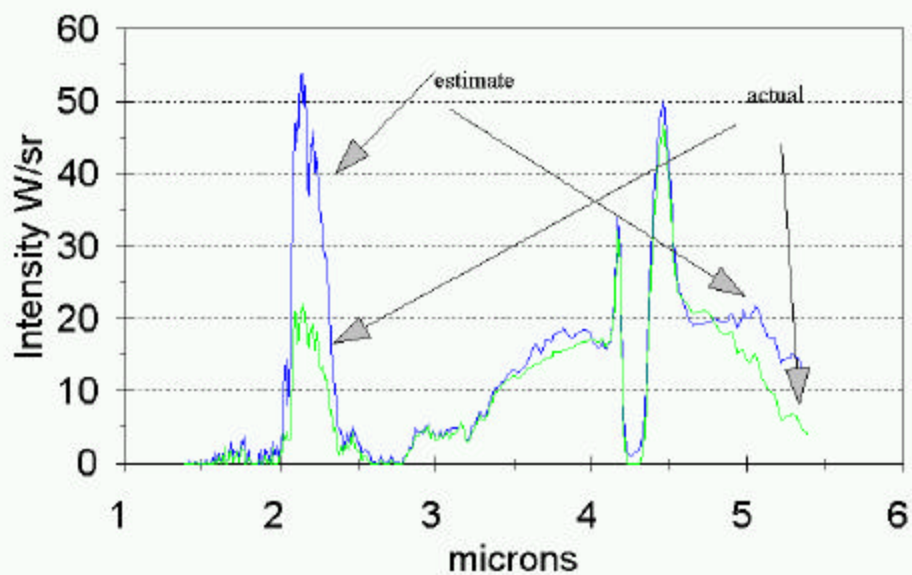


Figure 10

unclassified

Spectral Contrast

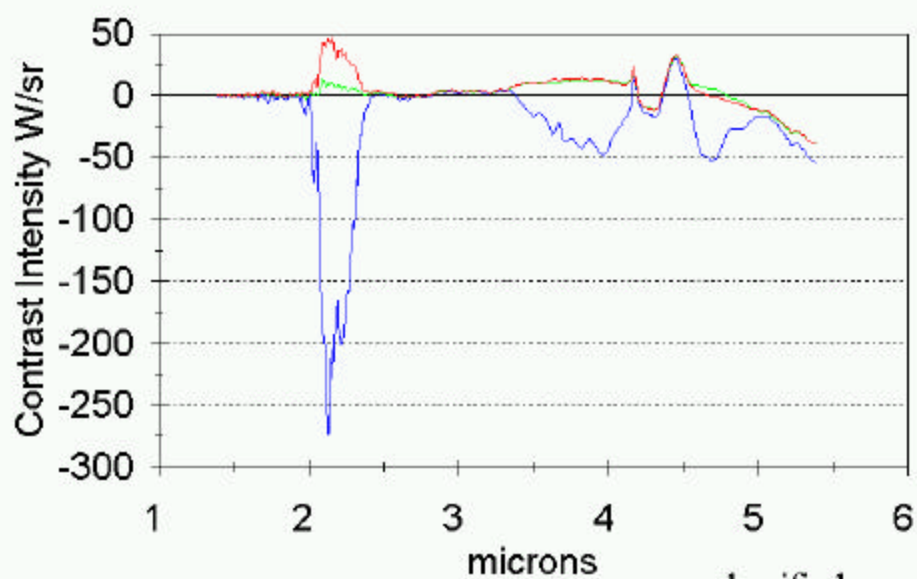


Figure 11a

unclassified

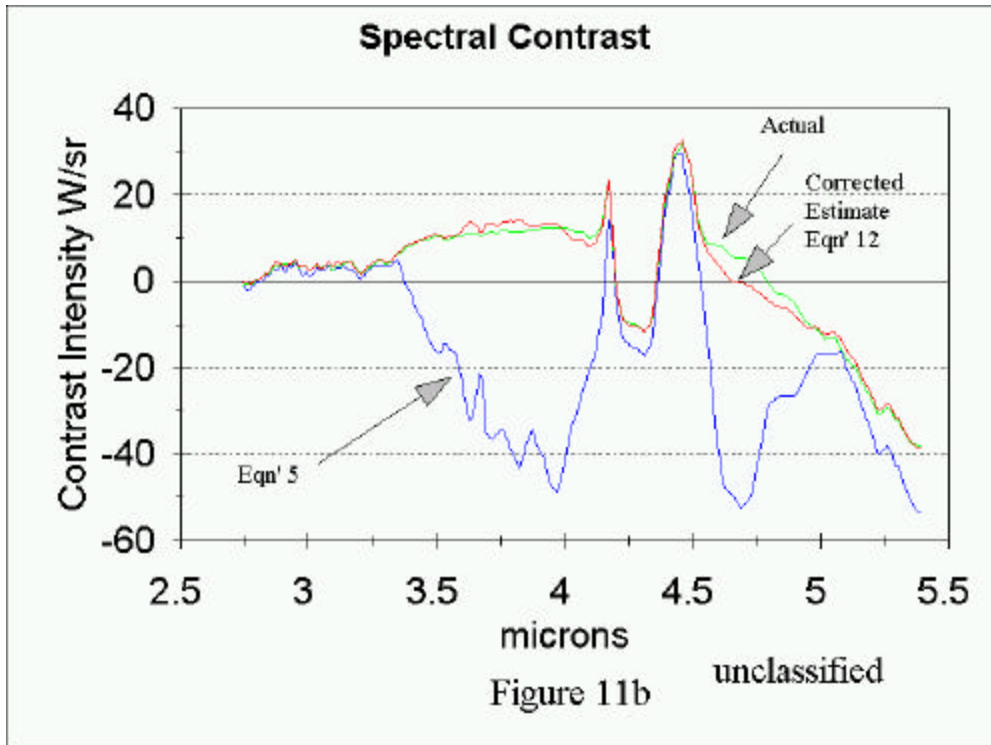
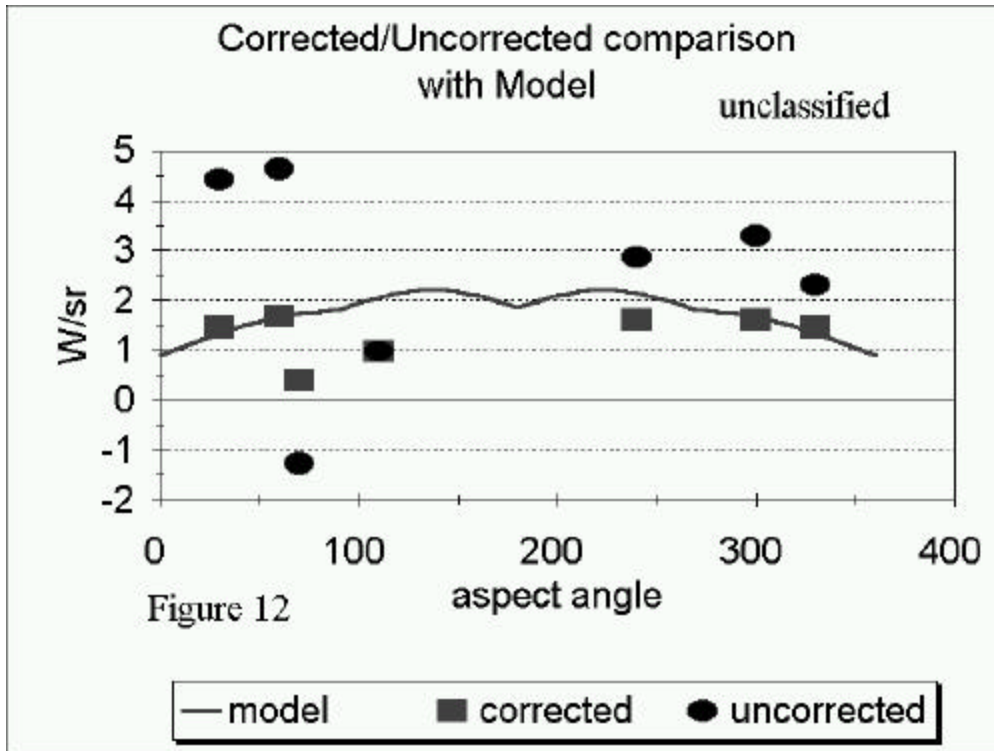


Figure 12 displays the measured spectra reduced to provide target estimates both with a correction for background variation and with no correction for background variation. The data is the result of integrating the resulting spectrum over the 3.8 to 4.7 micron band and plotting the result versus target aspect angle. The 110 degree aspect has both corrected and uncorrected data points since both estimates agreed at this aspect angle. Shown on the figure also is the results from a simple model of the aircraft as a function of aspect angle. The model was generated for a constant elevation angle while measurements were performed over a range of elevation angles as described earlier. Data shown is primarily for crossing runs due to difficulty in tracking such a small target on inbound and outbound trajectories.

We certainly cannot claim that the integrated intensity shown for the case where background variation has been corrected is superior to the uncorrected case because it agrees with an apriori model. It can be taken as an indication however that background variation can cause extreme deviation in resulting integrated spectral intensity (the data at 72 degrees actually is negative for the uncorrected case). We can state, that the corrected integrated values appear closer to what we expect, and that is often the final and only feedback when reporting measured spectral data taken in the field.



Conclusion

We have discussed the measurement of target and background spectra in field conditions and reviewed errors caused by the introduction of background variations. A simple technique has been introduced which corrects a portion of the background noise errors. The technique relies on estimating the amount of background obstruction and the ability to form an accurate estimate of the spectral shape of the background variation between the background in target field of view and that in the background-only measurement. Estimates of both the apparent target and contrast functions are obtained which are less susceptible to background variation errors. An example is provided to demonstrate the degree of correction which can be obtained in reducing background noise errors.

REFERENCES

1. Beer, R., "Remote Sensing By Fourier Transform Spectrometry", John Wiley and Sons Inc, New York (1992).
2. Herget, W.F., J.D. Basher, "Remote Fourier Transform Infrared Air Pollution Studies", *Optical Engineering*, 19, 508-514 (1980).
3. Chan, S. H., C.C. Lin, M.J.D. Low, "Analysis of Principles of Remote Sensing and Characterization of Stack Gases by Infrared Spectroscopy", *Env. Sci. and Tech.*, 7, 424-427 (1973).
4. Carlson, R.C., A.F. Hayden, W.B. Telfair, "Remote Observations of Effluents from Small building Smokestacks Using FTIR Spectroscopy", *Applied Optics*, 27, 4952-4959 (1988).
5. Compendium of Available Infrared Signature Data, Raytheon Missile Systems ,PO 11337, Tucson, AZ., 85734(1994).
6. Kroutil, R.T., J.T. Ditillo, W.R. Leorop, "Detection of Atmospheric Pollutants by Direct Analysis of Passive Fourier Transform Infrared Interferograms", *Analytical Chemistry*, 60, 264-269 (1988).
7. de Haseth, J. A., T. L. Isenhour, "Reconstruction of Gas Chromatograms from Interferometric Gas Chromatography/Infrared Spectrometry Data", *Analytical Chem.*, 49, 1977-1981 (1977).
8. Ludwig, C.B., W. Malkmus, G.N. Freeman, M. Slack, R. Reed. "A Theoretical Model for Absorbing, Emitting, and Scattering Plume Radiation", *AIAA Conf Thermophysics paper 81-1051*, 111-127 (1981).
9. Royer, A., N.T. P'Neill, A. Davis, L. Hubert, "Comparison of Radiative Transfer Models Used to Determine Atmospheric Optical Parameters from Space", *SPIE vol 928*, 118-135 (1988).
10. Hudson, R.D., "Infrared System Engineering", Wiley-Interscience , New York, 23-29 (1969).
11. PcModWin3 Manual , Ontar Corp., 9 Village Way, North Andover , MA., 01845 (1996).
12. "Background Spectral Radiance and Contrast In The Near-UV, Mid-IR and LWIR Regions", General Dynamics (now Raytheon) Radiation Technology Laboratory, TM6-125PH-438, (1976).
"Spectral Radiance Measurements of Natural Backgrounds ", General Dynamics (now Raytheon) Radiation Technology Laboratory, TM6-125PH-466, (1977).
13. Wollenweber, F.G., "Effects of Atmospheric Model Layering on LOWTRAN 6 Calculations of 8-12 μm Near-Horizon Sky Radiances", *NOSC TD 1193* (1988).
14. Maag, P.J., E.J. Parker, "Comparison of night sky spectral radiance measurements with MODTRAN and LOWTRAN 7 predictions", *SPIE vol 1687*, 187-198 (1992).

LIST OF FIGURES

Figure 1. Diagram of spectral background subtraction for optically thick and optically thin objects.

Figure 2 Typical spatial response pattern of a Fourier Transform Spectrometer showing azimuth and elevation variation of the spectral response of the instrument.

Figure 3. Measured sky background with reflected solar radiation at 2.0 to 2.5 μ . This measurement was taken in the fall at Yuma AZ.

Figure 4. Calculated path radiance for a winter desert atmosphere over a 3.5 km path length. Solar effects were not included in the calculation. Note the similarity between this figure and figure 3.

Figure 5. Photograph of an actual target showing the background associated with the target and one which would typically be considered a background field of view.

Figure 6. Measured variation between several spectra taken 30 degrees apart in azimuth at 2 degrees elevation of blue sky. The variation within one azimuth location is shown also for comparison.

Figure 7. Measured variation between several spectra taken 2.5 degrees apart in elevation in blue sky. Variation within the lower elevation angle is also shown.

Figure 8. Spectra representative of measured target and background showing target obstruction and background variation.

Figure 9, Actual mean square error and curve $\frac{f_e}{f_g}$. The value chosen for γ for this example was 1.3.

Figure 10. Estimated target spectrum (equation 11) and actual (equation 15) with the value of γ found in figure 9.

Figure 11. Normal spectral contrast function (equation 5), corrected spectral contrast estimate (equation 12), and actual spectral contrast functions. The value of γ was that found in figure 9.

Figure 12. Comparison of measured integrated spectral radiant intensity for a small model aircraft, and, similar data generated from a simple model. Data is shown for integrated spectra which have been corrected for background variation, and, for which no correction has been made.

Appendix A

The use of $\frac{\int e}{\int g} = 0$ to find the proper coefficient of the prototype correction is supported by two facts shown previously; the error curve is a relatively flat function of γ as shown in Figure 9, and, as shown in the example when spectra are given in units of intensity (W/sr) a good choice of the correction scale can be found in the vicinity of $\frac{\int e}{\int g} = 0$. The following discussion is meant to show why this choice is a workable solution, rather than present an in-depth validation of the metric.

The choice of correction is meant to minimize the mean square error between the actual target spectra and the estimate, or equivalently the mean square error between the background noise and the scale corrected prototype in as much as possible. Thus minimizing the function

$$A1 \quad \int (e - gP)^2 dI$$

would be minimized by the proper choice of the constant γ given the prototype P and the background noise e. Thus if the background noise were deterministically known (of course if it were deterministically known the measured data could be simply corrected without regard to prototypes)

$$A2 \quad g = \frac{\int e P dI}{\int P^2 dI}$$

a familiar result. If we rewrite equation 13 in terms of target (T), prototype (P), and, background noise (e) spectra,

$$A3 \quad e(g) = \frac{\int [T - Ae + AgP] P dI}{\int [T - Ae + AgP]^2 dI}$$

then $\frac{\int e}{\int g} = 0$ would imply

$$A4 \quad \left\{ \int [T - Ae + AgP]^2 dI \right\} \left(\int AP^2 dI \right) - \left(\int [T - Ae + AgP] P dI \right) \left(\int [T - Ae + AgP] 2AP dI \right) = 0$$

which has solutions

$$A5 \quad g = \frac{ep}{pp} - \frac{tp}{App} \pm \frac{\sqrt{A^2(ee \cdot pp - ep^2) + 2A(ep \cdot tp - et \cdot pp) + (pp \cdot tt - tp^2)}}{A \cdot pp}$$

where terms such as ep are the products of the two spectral functions integrated over wavelength

$$ep = \int e(I) \cdot P(I) dI$$

and similarly for the other terms. Analysis of A5 shows the right hand solution is close to what is desired form A2. There are deviations for target strength, for weak targets the solution is close, for strong targets the solution is too small. It must be remembered that for intense targets, the effects of background variation is less problematic than weak targets. A useful practical technique is to use the solution as calculated from A5 and perturb it with a small positive value until the final target spectrum satisfies the positivity constraint.

The correction for target strength must be monitored by looking at the resulting target spectrum in a region where it is known to be non-zero. Solar effects must be avoided since this technique does not correct for solar scattering variation effectively. Thus the spectrum must be monitored above approximately 2.5 microns. We employ the region 4.2 to 5 microns. In the event the resulting target spectrum is negative in this region, we add a small value to γ and reevaluate the target spectrum again (we move the solution to the right .02 each iteration). This process continues until the resulting target spectrum is non-zero in this region. This process of moving the solution to the right by a small increment is allowed because it is known the target spectrum is constrained to be positive and any reduction technique must produce results which are within this constraint. The exception is below approximately 2.5 microns since occasionally target spectra will show negative numbers due to solar effects in background subtraction. The process of constraining the target spectrum to be non-negative in a particular region can allow the noise prototype to have undue influence if the target strength is very weak (integrated values of $<.1$ W/sr in the mid infrared band) for typical noise prototypes. In this case, the target spectral shape will mirror the noise prototype and at such a point correction for background variation cannot produce a non-zero target spectra with a reliably accurate spectral shape.